

Electrochemical POC device for fast malaria quantitative diagnosis in whole blood by using magnetic beads, poly-HRP and microfluidic paper electrodes

Gisela Ruiz-Vega¹, Kevin Arias-Alpizar¹, Erica de la Serna¹, Livia Neves Borgheti-Cardoso^{2,3}; Elena Sulleiro⁴, Israel Molina⁵, Xavier Fernàndez-Busquets^{2,3,6}, Adrián Sánchez-Montalvá⁵, F. Javier del Campo⁷, Eva Baldrich^{1,8}.

¹ Diagnostic Nanotools Group, Cibbim-Nanomedicine, Vall Hebron Research Institute (VHIR), Universitat Autònoma de Barcelona (UAB), Barcelona, Spain

² Nanomalaria Group, Institute for Bioengineering of Catalonia (IBEC), The Barcelona Institute of Science and Technology (BIST), Barcelona, Spain

³ Barcelona Institute for Global Health (ISGlobal, Hospital Clínic-Universitat de Barcelona), Barcelona, Spain

⁴ Microbiology Department, Vall Hebron University Hospital (VHUH), UAB, Barcelona, Spain

⁵ Infectious Diseases Department, VHUH, UAB, PROSICS (Catalan International Health Program), Barcelona, Spain

⁶ Nanoscience and Nanotechnology Institute (IN2UB), Barcelona, Spain

⁷ Centro Nacional de Microelectrónica (IMB-CNM, CSIC), Barcelona, Spain

⁸ CIBER de Bioingeniería, Biomateriales y Nanomedicina (CIBER-BBN), Spain

ABSTRACT

Malaria, a parasitic infection caused by *Plasmodium* parasites and transmitted through the bite of infected female *Anopheles* mosquitos, is one of the main causes of mortality in many developing countries. Over 200 million new infections and nearly half a million deaths are reported each year, and more than three billion people are at risk of acquiring malaria worldwide. Nevertheless, most malaria cases could be cured if detected early. Malaria eradication of is a top priority of The World Health Organisation (WHO). This will require mass population screening and treatment, which will be hard to accomplish with current diagnostic tools.

We report an electrochemical point-of-care (POC) device for the fast, simple and quantitative detection of *Plasmodium* lactate dehydrogenase (pLDH) in whole blood samples. Sample

analysis includes 5-min lysis to release intracellular parasites, and agitation for 5 more min with immuno-modified magnetic beads (MB) along with an immuno-modified signal amplifier. The rest of the magneto-immunoassay, including sample filtration, MB washing and electrochemical detection, is performed at a disposable paper electrode microfluidic device. The sensor provides PfLDH quantitation down to 2.47 ng.mL^{-1} in spiked samples and for 0.006-1.5% parasitemias in *Plasmodium*-infected cultured red blood cells (RBC), and discrimination between healthy individuals and malaria patients presenting parasitemias $>0.1\%$. Quantitative malaria diagnosis is attained with little user intervention, which is not achieved by other diagnostic methods.

Keywords. Electrochemical magneto-immunosensor; paper microfluidic electrode; malaria quantitative diagnosis; *Plasmodium* LDH; point-of-care (POC) testing

1. Introduction

The availability of point-of-care (POC) testing devices for disease diagnosis near the patient is increasingly demanded by healthcare authorities, professionals and the population (Dincer et al., 2019). According to the World Health Organisation (WHO), POC devices should be ASSURED: Affordable, Sensitive, Specific, User-friendly, Rapid and robust, Equipment-free and Deliverable to end-users (Kosack et al., 2017). POC testing could improve disease diagnosis and management, providing a rapid diagnostic, reducing the time needed for treatment implementation, and facilitating treatment response monitoring. This makes POC testing an ideal technology for the diagnosis and surveillance of infectious diseases, especially in settings with limited infrastructure (Kozel and Burnham-Marusich, 2017; Zarei, 2018, 2017).

Malaria is an infection caused by the parasite *Plasmodium sp* and is transmitted by the bite of infected female *Anopheles* mosquitoes. There are five different species of *Plasmodium* that infect humans (*P. falciparum*, *P. vivax*, *P. malariae*, *P. ovale* and *P. knowlesi*), of which *P. falciparum* causes the most severe infections and the highest mortality (WHO, 2015a). More than three billion people are at risk of acquiring malaria, which in 2017 produced 219 million new infections (92% in Africa) and 435,000 casualties (WHO, 2018). Expanding the access to early diagnosis and treatment is one the most effective ways to prevent disease complications and severe cases, but this is hard to accomplish in resource-limited settings with the diagnostic methods currently available (Mathison and Pritt, 2017; Pham et al., 2018).

Light microscopy remains the gold standard diagnostic method, allowing for the species identification, parasitemia quantification, and staging of *Plasmodium*-infected RBC (Pham et al., 2018). However, light microscopy is time-consuming and requires trained staff and well-kept equipment, displaying cut-offs ranging between <10-50 and 100-500 parasites per μL of blood ($\text{p } \mu\text{L}^{-1}$), depending on the microscopist skills and experience (Ashley et al., 2018; Mathison and Pritt, 2017; McKenzie et al., 2003). On the other hand, molecular techniques such as PCR grant detection limits below 5 $\text{p } \mu\text{L}^{-1}$, but are time-consuming, expensive and need sophisticated installations and well-trained personnel (Hänscheid and Grobusch, 2002; Kasetsirikul et al., 2016). Finally, antigen RDT are affordable, simple to use, and produce results in 15-30 min that are interpreted visually without the need of any equipment (Mukkala et al., 2018). Nevertheless, RDT usually exhibit limited sensitivity (cut-offs $>100\text{-}200 \text{ p } \mu\text{L}^{-1}$), which hampers the identification of low parasitemias and asymptomatic patients (especially for *P. ovale* and *P. malariae*, which are often underdiagnosed) (Bridger et al., 2015). In addition, most RDTs display qualitative results and variability between devices, production batches, and users (Maltha et al., 2013; WHO, 2015b).

Strategies have been reported to improve malaria diagnosis (Kolluri et al., 2017; Pham et al., 2018; Ragavan et al., 2018). For instance, magneto-immunoassays have been optimized for detection of *Plasmodium falciparum* histidine-rich protein 2 (HRP2) and *Plasmodium* lactate dehydrogenase (LDH) using magnetic beads (MB) and colorimetric (Markwalter et al., 2016b, 2016a), fluorescent (Kim and Searson, 2017) or electrochemical detection (De Souza Castilho et al., 2011). However, MB are sequentially incubated under agitation and washed using magnets, which is hard to integrate into a low-cost POC device. Microfluidics can be used to automate such analytical procedures, but usually employing relatively complex microvalves, micromixers or micropumps. A notable exception are microfluidic paper analytical devices (μPADs) (Mahato et al., 2017; Salentijn et al., 2018). μPADs exploit passive capillarity pumping and hydrophobic patterns to define channels and chambers. Examples of two and three-dimensional colorimetric μPADs have been reported for *Plasmodium* detection (Deraney et al., 2016; Fridley et al., 2014; Fu et al., 2012; Pereira et al., 2015).

Here, we present the development of an electrochemical POC device for the fast, simple and quantitative detection of *Plasmodium falciparum* LDH (PfLDH) (Jain et al., 2014). This POC entails an optimized single-step immunoassay, performed with MB and an immuno-modified signal amplifier, which is mostly carried in a single-use microfluidic paper double-sided screen-printed carbon electrode (MP-dsSPCE). As we show, the sensor affords quantitative detection in whole blood samples in <20 min with minimal user intervention, which is unafforded by most RDT.

2. Material and Methods

2.1. Reagents and biocomponents

Recombinant PFLDH was provided by CTK Biotech (San Diego, USA). Anti-PLDH monoclonal capture and detection antibodies (c-MAb and bd-MAb) were from BiosPacific (California, USA). Carboxylic acid MB (MyOne, 1 μ m diameter, Ref. 65011), Streptavidin Poly-HRP (Ref. 21140) and EDC (1-ethyl-3-(3-dimethylaminopropyl) carbodiimide hydrochloride) were from Thermo Fisher (Waltham, USA). Bovine serum albumin (BSA), Tween 20, potassium hexacyanoferrate (II), and 2-(N-morpholino)ethanesulfonic acid (MES) hydrate were from Sigma-Aldrich (Madrid, Spain). Phosphate-buffered saline tablets (PBS; Gibco) produced 10 mM sodium phosphate, NaCl 140 mM, KCl 2.7 mM, pH 7.4. Reagent Diluent (10 \times RD, equivalent to PBS, 10% BSA) was from R&D (Abingdon, UK). **A commercial ready-to-use enzyme substrate solution was used for the spectrophotometric and electrochemical detection of the magneto-immunoassays (Ref. T0440, Sigma-Aldrich). This solution contained hydrogen peroxide (H₂O₂) and 3,3',5,5'-tetramethylbenzidine (TMB) at unrevealed concentrations in an acidic buffer (pH 3.50-3.90) of undisclosed composition. This product was stable for months at 4°C and was used as received, without being diluted or modified in any way.**

2.2. Fabrication of the MP-dsSPCE and electrochemical measurements

MP-dsSPCE were designed using Vectorworks 2017, Student Edition (Techlimits, ES). Each device contained a Ag pseudo-reference electrode (RE), and double-sided graphite working (WE) and counter electrodes (CE) (Figure S-1). Screens, 25 \times 25 cm/21 \times 21 cm (outer dimensions/inner dimensions), were outsourced from Paymsar (ES). MP-SPE were produced on Fusion 5 (GE Healthcare, Dassel, Germany) (Ruiz-Vega et al., 2017). Carbon paste C2030519P4 (Gwent Electronics, UK) was used for printing the WE and CE. Silver paste Electrodag™ 725A (Henkel, ES) was used to print the RE, tracks and contact pads. UV-curable dielectric Electrodag™ PF-455B/BC (Henkel, ES) was used to insulate the silver tracks. 16 chips (10 \times 20 mm) were printed per production batch through a process involving 8 printing steps (Figure S-2).

Electrochemical measurements were performed employing a DropSens μ Stat 8000 multipotentiostat and DropView 8400 software (DropSens, Spain). Commercial SPCE (DRP-110; Dropsens, Spain) were used as reference material. Before their utilization, SPCE were rinsed with 70% ethanol and water, dried under an airflow, and characterized by cyclic voltammetry (CV) in 0.1 M H₂SO₄, 25 mM K₄Fe(CN)₆.

2.3. PFLDH magneto-immunodetection

2.3.1. MB modification with c-MAb. MB were immunomodified based on a protocol optimized previously (Ruiz-Vega et al., 2018). Briefly, MB (20 µg in 200 µL) were washed twice with 15 mM MES using a magnetic separator (BILATEST, Sigma Aldrich). MB were next agitated for 2 h with 50 µg of c-MAb in 100 µL of 4 mg mL⁻¹ EDC (600 rpm, Vortex Genie 2, Scientific Industries, Bohemia, USA). After that, MB were serially washed with 200 µL of MES and PBS, and blocked for 1 h with PBS, 1% BSA (PBS-BSA_{1%}). The c-MAb-MB were then washed twice for 5 min with 100 µL of PBS, 0.1% Tween 20 (PBST) and resuspended in 1 mL of PBST, 0.2% BSA (PBST-BSA_{0.2%}) for storage at 4 °C (1.4-2.4×10⁹ MB mL⁻¹, equivalent to 2 mg mL⁻¹).

2.3.2. Modification of Poly-HRP with bd-MAb. An immuno-modified Poly-HRP conjugate (bd-MAb/Poly-HRP) was produced as in (Ruiz-Vega et al., 2018) by incubating Poly-HRP (10 µg mL⁻¹) with bd-MAb (45 µg mL⁻¹) in PBS, 0.1% BSA (PBS-BSA_{0.1%}), for 60 min at room temperature (rotation at 24 rpm). This bd-PAb/Poly-HRP conjugate was then rotated for 30 min with free biotin (4.88 mg mL⁻¹ in PBS) and stored at 4 °C. The conjugates were stable at 4°C for 1 month and the variability between production batches was below 10% (Figure S-3).

2.3.3. PflDH single-step sandwich magneto-immunoassay. Before their utilization, c-MAb-MB were washed twice with PBS and resuspended in 1×RD to 5 mg mL⁻¹. PflDH was then stirred for 5 min at 600 rpm, in 100 µL of 1×RD with 4 µL of c-MAb-MB and 0.5 µL of bd-MAb/Poly-HRP (final concentration of 225 ng mL⁻¹ of bd-MAb and 50 ng mL⁻¹ of Poly-HRP).

For assay spectrophotometric detection, MB were washed twice with 150 µL of PBST, resuspended in 100 µL of TMB substrate solution and stirred for 20 min at room temperature in the dark. After terminating the reaction with 50 µL of 1 M sulphuric acid, MB were concentrated, the supernatant was transferred to 96-well non-binding plates (Corning® NBS™), and absorbance was measured at 450 nm using a Sunrise plate reader (Tecan, Switzerland).

For electrochemical detection, MB were resuspended in 50 µL of PBS and confined onto the WE using a customized 8× multiplexed magnetic holder (Ruiz-Vega et al., 2018). Current was stabilized at 0 V vs. Ag for 150 s, the measurement was paused, PBS was substituted by TMB substrate solution and the amperometric measurement was resumed for other 150 s.

For electrochemical detection using MP-dsSPCE, after the 5-min incubation, the mixture containing PflDH, c-MAb-MB and bd-PAb/Poly-HRP was directly pipetted onto the paper surface. MB were retained using a neodymium magnet and four consecutive washes were carried by adding 100 µL of PBST each time, while current was registered at -0.05 V vs. Ag for 300 s. TMB enzyme substrate solution (100 µL) was finally added and current was monitored amperometrically for other 150 s.

In all cases, Poly-HRP catalysed the reduction of H₂O₂ coupled to TMB oxidation. The resulting oxidised TMB was then either measured spectrophotometrically or reduced at the electrode surface for electrochemical detection.

2.3.4. PfLDH detection in cultured *P. falciparum* and whole blood clinical samples

The method developed was initially tested in cultured *P. falciparum*, grown at 37°C with human RBC following standard protocols as detailed in the Supplementary Material (Ljungström et al., 2008). For culture maintenance, parasitemias were kept below 5% by dilution with fresh RBCs. For standard assays, the culture was maintained under agitation for 3-5 days, when parasitemia was adjusted with >90% of parasites synchronized at ring stage. *Plasmodium* culture parasitemias ranging from 0.0058 to 1.5% (45% haematocrit) were then obtained by serial dilution of the initial culture with fresh RBC and medium. Parasitemia of the initial culture was determined by flow cytometry (Moles et al., 2015) and the different culture dilutions were characterized by real-time PCR (Mayor et al., 2009).

For the study of patient samples, peripheral blood was drawn in heparin collection tubes before the administration of any antimalarial drugs. Malaria acute infections were confirmed by microscope blood examination and/or by PCR (Rougemont et al., 2004). The Ethics Committee of Vall d'Hebron University Hospital approved the study (PR(AG)30/2018) and informed consent was signed by all patients.

For detection of PfLDH using the magneto-immunosensor, samples were diluted 1:1 with lysis buffer (50 mM KH₂PO₄, 300 mM NaCl, 0.25 M imidazole, 1% Triton X-100), incubated for 5 min at room temperature, diluted 1:25 with 1×RD, and processed as described in section 2.3.3. All samples were analysed 3 times independently and studied in parallel by ELISA and optical microscopy (Figure S-4).

2.4. Data analysis

The limits of detection (LOD) and quantification (LOQ) were calculated as the average of the blanks plus 3 and 10 times their standard deviation (SD), respectively. The sensitivity corresponded to the slope of the assay linear range. The variability was calculated in terms of coefficient of variation (% CV = (SD/mean) × 100). The signal-to-noise ratio (S/N) corresponded to the signal registered for each PfLDH concentration divided by the signal from the blanks. PfLDH recovery corresponded to the amount of PfLDH detected by the magneto-immunosensor compared to the ELISA reference method (% Recov = ([PLDH]_{MBassay}/([PLDH]_{ELISA}) × 100).

3. Results and discussion

Combining MB and signal amplifiers, such as Poly-HRP (a polymer that includes between tens and hundreds of molecules of peroxidase conjugated to streptavidin), allows producing fast, simple and efficient magneto-immunoassays (Ben Ismail et al., 2018). Nevertheless, magneto-immunoassays entail serial washing steps using magnets and removal and addition of reagents, which is hard to carry out by inexperienced personnel. Previously, we employed a microfluidic paper single-sided SPCE (MP-ssSPCE) to perform on-chip MB washing and detection, demonstrating myeloperoxidase magneto-immunodetection with little user intervention (Ruiz-Vega et al., 2017). Here we report on an upgraded double-sided device (dsMP-SPCE) that provides higher detection efficiency.

3.1. Production and characterization of the MP-dsSPCE

MP-dsSPCE, depicted in Figure 1, featured WE and CE on both sides of the paper, plus a RE on one of them. The large WE active area offered efficient detection of the flowing electroactive species. The entire device surface was protected by a water-proof dielectric, except for the laser-cut edges and the centre of the ring-shaped top WE. This circular opening allowed the entry of MB and solutions into the paper matrix. The frontal edge, on the other hand, was connected to an adsorbent that provided solution draining and waste storage. Thus, MP-dsSPCE could be used alternatively to carry electrochemical measurements under static and flow conditions (Figure S-5).

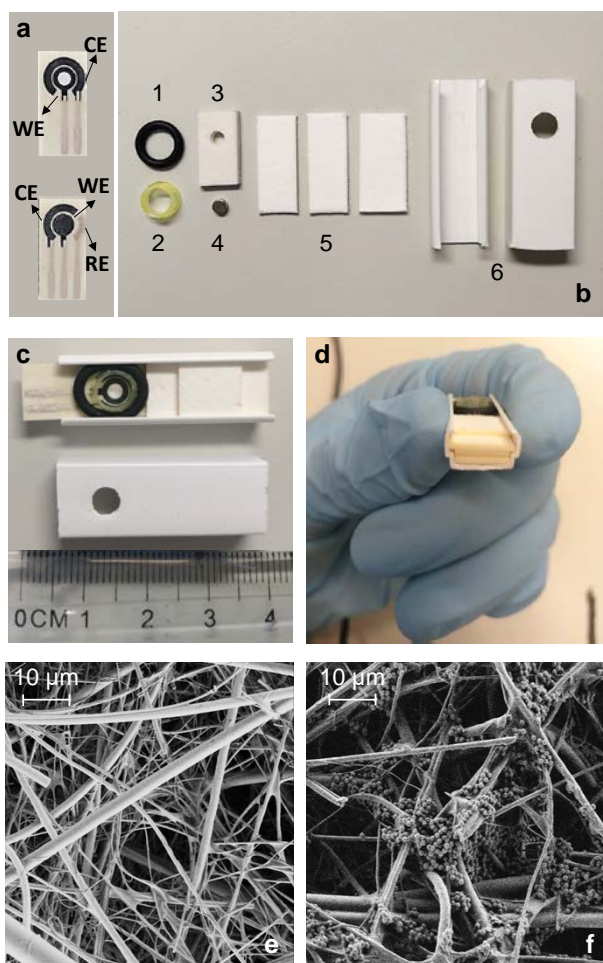


Figure 1. Production of the MP-dsSPCE POC device. a) Top and bottom sides of the MP-dsSPCE. b) Device components: (1) o-ring, (2) segment of a pipette tip, (3) silicon sheet with a perforation for the magnet (4), (5) absorbent pads, and (6) square cable trunking section. c-d) Assembled MP-dsSPCE and detail of the pile of absorbent pads. e-f) SEM images of a transversal cut of the MP-dsSPCE carried out before (d) or after (e) MB magnetic confinement and wash.

MP-dsSPCE were connected to the potentiostat using a standard 2.54 mm pitch connector. Previous immersion of this chip edge in 15 μL of a transparent impermeabilizing solution (Rubson SX9000, Henkel, Germany) created a hydrophobic barrier that protected this zone from the flowing solutions (Figure S-6).

The MP-dsSPCE were characterized by CV in ferrocyanide using alternatively the top, bottom and top-bottom cross circuited WE/CE (Figure 2a-b). While under static conditions top and bottom WE displayed similar performance, the bottom electrodes registered significantly lower currents, larger peak-to-peak separation and more negative overpotentials under flow conditions. This confirmed that solution flow compromised detection using electrodes at the bottom of the chip. In spite of this, using top-bottom cross-circuited WE provided higher currents compared to using only the top WE, suggesting that this was the best electrode

arrangement. Furthermore, the CVs obtained with the MP-dsSPCE had peaks 20 times higher than those detected by the previous version described in (Ruiz-Vega et al., 2017) and close to those observed for commercial SPCE (Figure 2c).

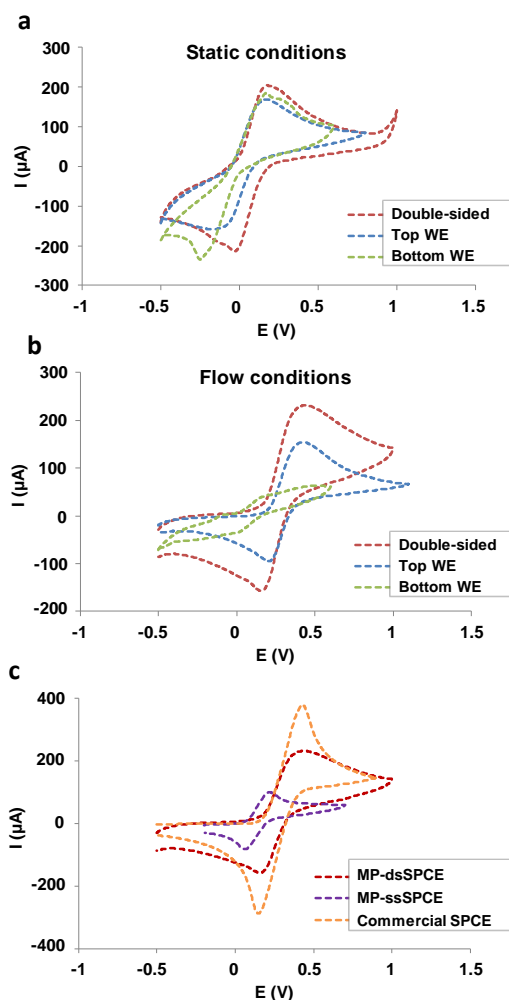


Figure 2. Characterization of the MP-dsSPCE. (a,b) CVs obtained in 25 mM of ferrocyanide in 0.1 M H_2SO_4 (50 mV s^{-1}) at MP-dsSPCE, using alternatively the top, bottom and top-bottom cross-circuited WE and CE. (a) static conditions. (b) flow conditions. (c) Comparison of the CVs registered with the MP-dsSPCE, the MP-ssSPCE reported in (Ruiz-Vega et al., 2017) and a commercial SPCE.

3.2. Low-cost POC device for magneto-immunoassay electrochemical detection

In order to perform most of the steps of a magneto-immunoassay on-chip, including serial MB magnetic confinement, washing and electrochemical detection, the MP-dsSPCE was inserted in a 4.5-cm segment of PVC electrical cable trunking (45×12×0.7 mm; SevenOn elec, Hidalgo's Group, Spain), which served as the platform holder (Figure 1). A perforated piece of silicone elastomer (15×8×2 mm; GoodFellow, England) allowed embedding a neodymium magnet (3 × 1.5 mm; IMA, Spain), which lied below the WEs. A ring cut from the bottom of a polypropylene

pipette tip (4 mm high, 5 mm \varnothing ; Nirco, Spain) was placed on the electrochemical cell to prevent solution spreading. Finally, a Viton o-ring (6.1 mm internal \varnothing , 9.5 mm external \varnothing , 1.78 mm wall thickness; Sigma Aldrich) kept all the components in place. Once closed, the holder displayed a window that granted access to the electrodes for solution transfer. When a MB suspension was pipetted, the solution flowed through the top WE orifice and into the paper matrix, while MB were retained by the magnet. As illustrated in Figure 1e-f, MB remained in place even after extensive washing under flow conditions.

The MP-dsSPCE absorbed only 85 μL of solution. For this reason, an external absorbent pad was incorporated to the system that provided additional absorption capacity for sample and reagents. Nine types of commercially available membranes were evaluated for this purpose (Figure S-7) (GE Healthcare Bio-Sciences, 2013). Among them, CF5 provided the highest water absorption capacity (99.2 mg cm^{-2}) and most uniform capillary flow rate (Figure S-8).

3.3. Electrochemical detection of PflDH using MB and MP-dsSPCE

PflDH detection was accomplished by optimizing a single-step sandwich immunoassay (Figures S-9 and S-10). Figure 3 illustrates schematically the different assay versions developed, which will be described below.

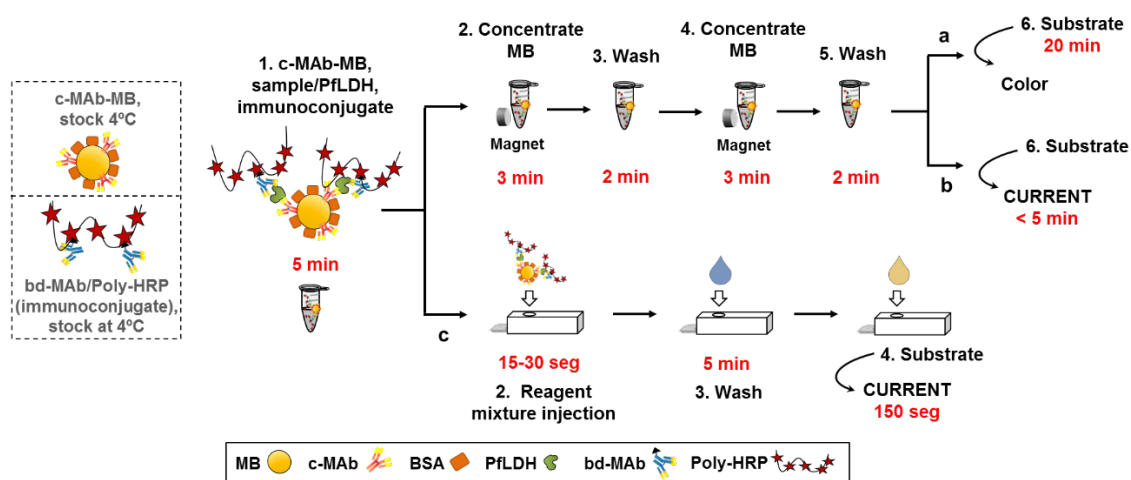


Figure 3. Different formats of the single-step magneto-immunoassay. a) Spectrophotometric detection. b) Electrochemical detection using SPCE. c) Electrochemical detection at a MP-dsSPCE, with washes and detection performed on-chip.

3.3.1. Optimization of a single-step magneto-immunoassay for PflDH detection

The single-step magnetoimmunoassay consisted of a simultaneous 5-min incubation of the sample with c-MAb-MB and bd-MAb/Poly-HRP immunoconjugate. Figure 3a represents the classical approach, in which MB were then washed twice with PBST using a magnetic rack,

incubated for 20 min with TMB substrate solution, concentrated, and the supernatant was finally transferred to a microtiter plate for spectrophotometric detection. Figure 3b corresponds to the amperometric counterpart, in which MB were resuspended in PBS after the last wash, and were confined with a magnet on a commercial SPCE for electrochemical detection of the enzyme label in TMB substrate solution. The colorimetric assay exhibited linear response for PflDH concentrations ranging 0.4-25 ng mL⁻¹, with LOD/LOQ of 0.48 ng mL⁻¹ and 1.72 ng mL⁻¹, respectively. The electrochemical magneto-immunosensor displayed linear response between 3-100 ng mL⁻¹ and LOD/LOQ of 0.58 ng mL⁻¹ and 2.48 ng mL⁻¹.

In both cases, while the single immunocapture took 5 min, each washing step required (i) MB concentration in the magnet for 3 min, (ii) supernatant removal by pipetting without disturbing the MB sediment, (iii) MB resuspension in PBST and incubation under rotation for 2-5 min, and (iv) new concentration in the magnet for 3 min for the removal of the washing buffer. These washes were time consuming, tedious, and an important source of result variability, especially for poorly trained users. The objective of this work was performing the washing and detection steps of the magneto-immunoassay on-chip in a way as simple as possible (Figure 3c).

3.3.2. Optimization of the electrochemical detection using MP-dsSPCE

Initially, the whole assay was performed in tubes and only detection was carried out on-chip. For this, after the last wash, MB were resuspended in TMB substrate solution and pipetted onto the MP-dsSPCE. The amperometric measurement was then carried out at different measurement potentials, either under static or flow conditions. In general, the currents and S/N ratios registered were lower under flow conditions, which was attributed to enzymatic substrate flow along the MP-dsSPCE before being detected (Godino et al., 2010). The best measurement potential was -0.05 V in both cases, which provided the highest S/N (Figure S-11a,d). On the other hand, flow detection benefited from using larger TMB volumes, which permitted extending the measurement and generating higher currents, although not better S/N (Figure S-11b,e).

Electrochemical detection under static conditions produced comparable currents and S/N when the assay was performed with 10, 15 or 20 µg of MB per sample, but result reproducibility improved with MB load (%CV of 19.27%, 12.68% and 5.63%, respectively) (Figure S-11c,f). This was presumably caused by more efficient magnetic retention of higher MB loads during the incubation and washing steps performed in tubes (Ruiz-Vega and Baldrich, 2017). The effect of MB concentration was clearer under flow measurement conditions, for

which both current and S/N increased with the amount of MB (%CV of 17.69%, 13.55% and 8.17% for 10, 15 and 20 MB μg , respectively).

3.3.3. Optimization of MB on-chip washing and detection using MP-dsSPCE

To wash and detect MB on-chip, the mixture of sample, MB and reagents was directly transferred to the MP-dsSPCE after the 5-min incubation in tubes. Then, two consecutive injections of 100 μL of PBST were done to wash the MB, while current was allowed to stabilize for 300 s. Finally, 100 μL of TMB were added and current was monitored for a further 150 s. As before, the currents registered increased as the measurement potential shifted to more negative values, but the background noise raised as well (Figure 4a). The best S/N ratios were attained at -0.05 V, which provided also the lowest LOD/LOQ.

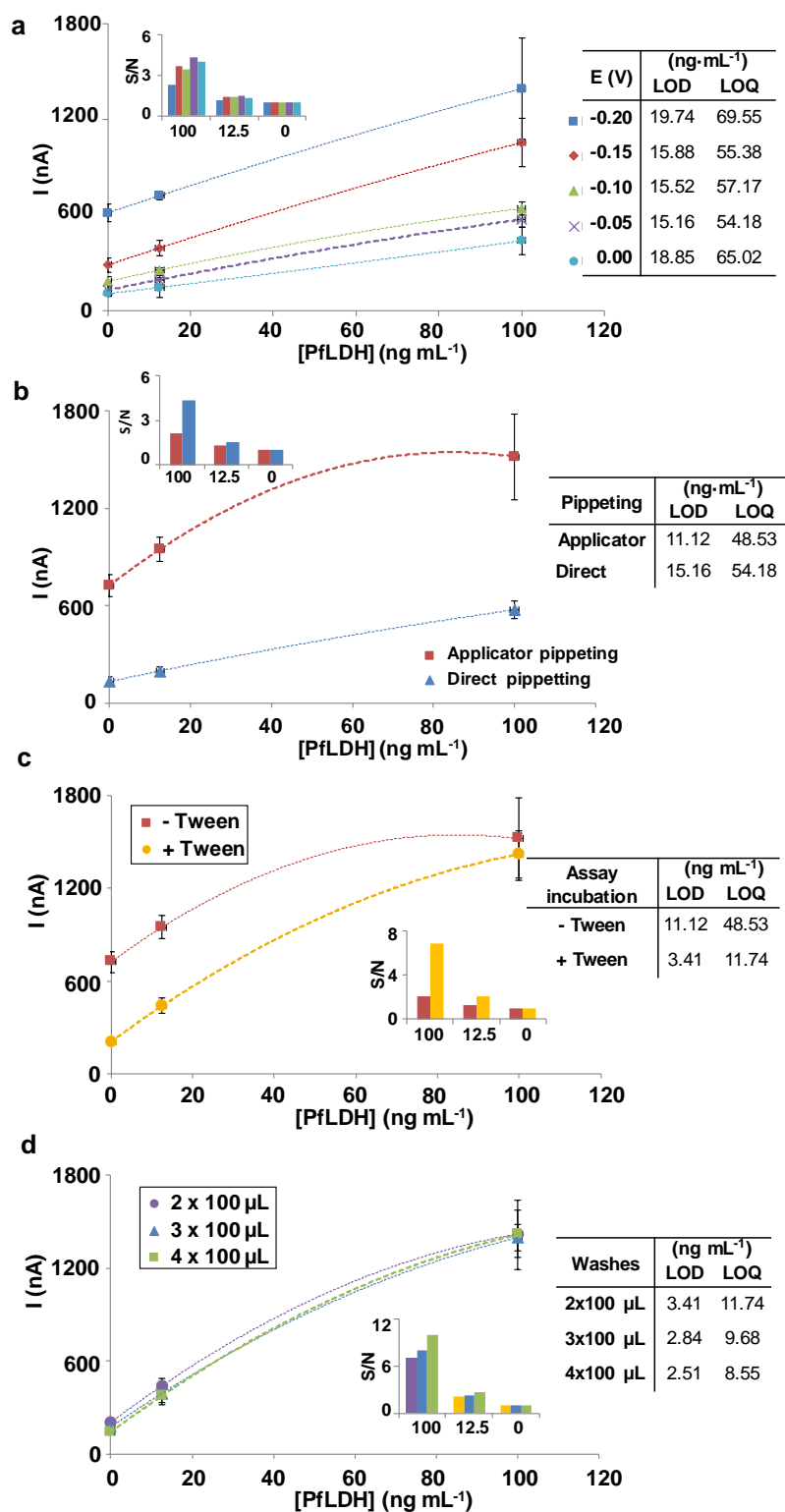


Figure 4. Optimization of MB washing and detection on-chip using MP-dsSPCE. Effect of measurement potential (a), solution injection procedure (b), addition of 0.05% Tween 20 to the incubation buffer (c), and number of serial washing steps (d) in magneto-immunoassay electrochemical detection.

Solutions pipetted directly on the MP-dsSPCE flowed relatively fast (100 μ L took 30 s to enter the paper), which contributed to the low currents registered under flow measurement

conditions. For this reason, a conical channel was incorporated between the electrochemical cell and the holder window (component 2 in Figure 1). When the holder was closed, this fitting facilitated solution positioning onto the electrodes, prevented liquid spreading, and applied a mild pressure onto the MP-dsSPCE, slowing solution flow rate. This extended the enzymatic reaction time from 50 to 150 s, providing higher currents and lower LOD/LOQ (Figure 4b).

Nevertheless, the new flow conditions produced also significantly higher background noise, which was attributed to worse MB washing efficiency. This issue was compensated by including a detergent in the single-step incubation buffer. As Figure 4c shows, carrying the assay in 1×RD supplemented with 0.05% Tween 20 provided currents 3.5 times lower for the blanks than when preparing the samples in 1×RD only. In contrast, the currents registered in the samples containing PfLDH were comparable in both cases. As a result, S/N improved when using detergent, as did LOD/LOQ too. Figure 4d shows that increasing the number of consecutive washing steps from 2 to 4 (100 µL of PBST each) did not change the results drastically. Nevertheless, the mild improvement in background noise allowed improving S/N, achieving an LOD of 2.51 ng mL⁻¹ and an LOQ of 8.55 ng mL⁻¹.

3.4. Detection of PfLDH in lysed whole blood

The magneto-immunosensor was finally used to study lysed whole blood. For this study, blood from a healthy volunteer was obtained in parallel in collection tubes with three different anticoagulants, EDTA, heparin and citrate, or no anticoagulant at all. These samples were then assayed using the single-step magneto-immunoassay, before and after spiking 100 ng mL⁻¹ of PfLDH. Only EDTA interfered significantly in assay performance, producing in the negative controls (without PfLDH) signals as high as those in the presence of PfLDH (Fig. S-12). In contrast, EDTA did not affect the multi-step ELISA, in which extensive washing was carried before PolyHRP addition. Since EDTA is a chelating agent, interference could be caused by EDTA complexation with iron atoms from the PolyHRP, forming EDTA-iron complexes that could display peroxidase mimetic activity [REFS]. On the other hand, blood samples obtained in heparin collection tubes were those producing the lowest background noise and higher S/N ratios (Figure S-12). Accordingly, heparin was used in subsequent experiments.

Immediately before the analysis, RBC were lysed to release intraerythrocytic parasites. However, if lysed blood was directly pipetted on the MP-dsSPCE, some sample components attached to the paper that were not removed by on-chip washing. This raised the background noise and worsened the sensor LOD/LOQ. In order to protect the MP-dsSPCE, a filtration unit was incorporated (Figure 5a and S-13). This was a Fusion 5 strip (30×10 mm) with a protruding star-like fringe that rested onto the WE. This element prevented sample entry into the MP-

dsSPCE by directing the flow towards the main body of the filtration unit, which acted as both flow pump and waste container. Once the mixture of sample and reagents had been adsorbed, the main body of the filtration unit was pulled out, leaving the star-like section with the MB over the electrochemical cell (Figure 5a).

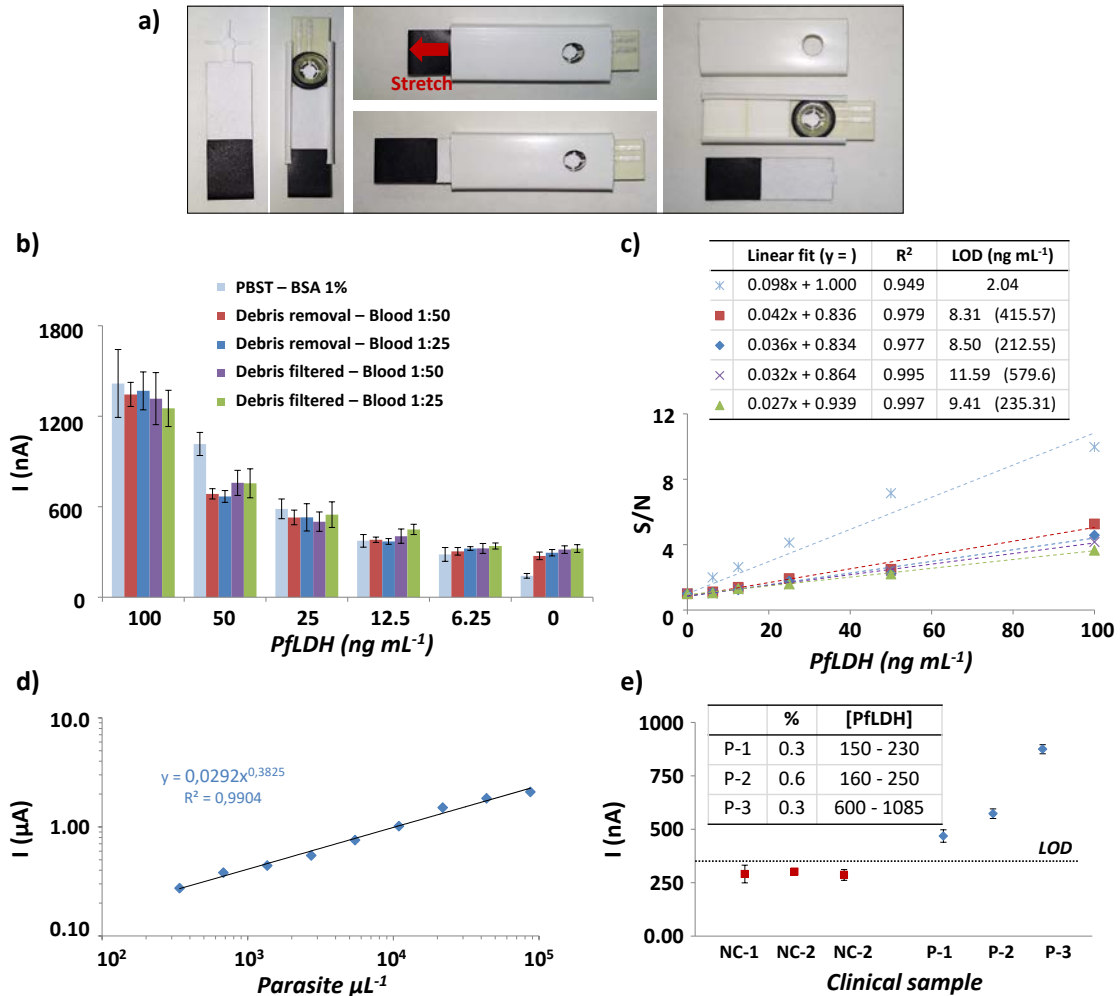


Figure 5. Detection of PflDH in whole blood. a) From left to right, filtration unit before and after assembly in the holder, procedure for module release after sample filtration, and device after filtration unit release. b) Signals registered for PflDH spiked in lysed whole blood. Cell debris and reagent excess were removed alternatively using a magnetic rack previous to injection in the MP-dsSPCE, or by on-chip filtration. c) S/N ratios, fitting equations and LODs of the assays in (b). LOD refers to PflDH concentration spiked in diluted blood and values in brackets indicate the corresponding pre-dilution concentration. d) Currents registered by the MP-dsSPCE for RBC cultures infected with controlled *P. falciparum* parasitemias. e) Detection of clinical samples obtained from malaria patients malaria and healthy volunteers. (Insert) Parasitemias (%) and PflDH concentrations (ng mL⁻¹) obtained by microscopy and ELISA, respectively, for the 3 patient samples (P-1 to P-3). **The graphs show averages of no less than 3 independent replicates and their standard deviations.**

The applicability of the MP-dsSPE was first tested in spiked lysed whole blood. For these experiments, pooled human blood was lysed for 5 min, diluted 1:50 or 1:25 with PBST-BSA, and spiked with increasing concentrations of PfLDH. Interference in the electrochemical detection was prevented through two alternative strategies (Figure 5b). First, after the 5-min incubation of the sample with MB and reagents, the tubes were placed in the magnetic rack for MB confinement and the supernatant containing cell debris was removed. MB were then resuspended in 100 μL of PBS and injected in the MP-SPE to perform the washes and the electrochemical detection on-chip. Alternatively, the mixture of spiked lysed blood, MB and reagents was directly pipetted on the MP-dsSPCE filtration unit. Once the solution had been adsorbed, the filtration unit was pulled out, and on-chip washing and detection proceeded as before. Interestingly, the currents registered for the two pre-treatments were comparable (Figure 5b). Although the negative controls were twice higher in lysed whole blood than in PBST-BSA, which worsened the assay S/N, LOD and sensitivity, the sensor linear response spanned between 6.25 and 100 ng mL^{-1} in all cases (Figure 5c). **Furthermore, result variability was below 15% for all the concentrations of PfLDH tested (n=3), and only slightly higher for on-chip blood filtering (%CV 6-12 %) than for sample removal by pipetting using a magnetic rack (5-11%) (Figure S-14).** This demonstrated that MP-dsSPCE could be used in whole blood and that the filtration unit provided efficient sample pre-treatment with less handling than the classical approach. Furthermore, the sensor displayed an LOD of 8.5 ng mL^{-1} in lysed blood diluted 1:25, which was equivalent to a predilution PfLDH concentration of around 200 ng mL^{-1} . While most commercial RDT detect *Plasmodium falciparum* HRP II, an antigen not produced by the other human-infecting species, displaying LODs in the range of 0.4-1.6 ng mL^{-1} , the few devices that detect LDH exhibit LODs spanning 10-1000 ng mL^{-1} (Jimenez et al., 2017). The magneto-immunosensor had an LOD of this order, providing also quantitative detection in the whole detection range tested.

The sensor was next tested on *in vitro Plasmodium*-infected RBC cultures with controlled parasitemias spanning 0.0058-1.5%, equivalent to 340-87209 parasites μL^{-1} . Samples were lysed for 5 min, diluted 1:25 with PBST-BSA_{1%} and studied using the MP-dsSPCE. The sensor detected PfLDH in the whole dilution series (Figure 5d), displaying an LOD around 300 parasites μL^{-1} . This value is close to the threshold recommended by the WHO, 200 parasites μL^{-1} , which is below the mean parasite density found in many populations in areas with endemic malaria (WHO, 2015b). Besides, the concentrations of PfLDH estimated by the MP-dsSPCE correlated linearly with those provided by the reference ELISA and by the magneto-immunosensor using classical washes in tubes and detection with commercial SPCE (Figure S-15). Furthermore, PfLDH detection was more sensitive than that provided by one of the

commercial RDT recommended by the WHO, which only provided faint LDH detection for culture parasitemias above 1.5% (equivalent to >87209 parasites μL^{-1} ; [Figure S-16](#)).

The sensor was finally employed to study 6 real blood samples, three from malaria patients and 3 from healthy volunteers. The currents registered for the two types of samples were below and above the LOD calculated for the sensor in spiked lysed whole blood, respectively. **In addition, the quantification provided by the sensor was consistent with the range of PfLDH concentrations detected by classical ELISA (insert in [Figure 5e](#)).** Although a higher number of samples will have to be tested in the future, these results suggest that the assay and device developed could provide PfLDH-based diagnosis of mid-to-high malaria parasitemias with little handling by the user, LOD comparable or better than those exhibited by most RDTs, and quantitative detection over the whole assay range.

4. Conclusions

A POC device has been developed that included a MP-dsSPCE produced by double-sided screen printing, a magnet, a whole-blood filtration unit and absorbent pads assembled into a low-cost customized cartridge. The system has been employed for PfLDH detection using a single-step magneto-immunoassay with little intervention of the user. This was achieved by optimizing an extremely simple magneto-immunoassay path, which operation was mostly performed on-chip. As we have shown, the system detected PfLDH in lysed whole blood in <20 min, providing an LOD of 200 ng mL^{-1} (equivalent to 300 parasites μL^{-1} , which is close to the WHO recommendations for clinical malaria diagnosis), and parasitemia quantitation in a wide range (0.006-1.5% in cultured RBC). Compared to the commercial RDTs that detect *Plasmodium* LDH, our POC prototype provided a similar level of manipulation, comparable or better LOD, but also infection objective quantification. These results suggest that paper microfluidics can be exploited to simplify magneto-immunoassay handling, taking MB closer to the requirements of POC testing.

Acknowledgements

This work has been supported by grants (i) CPII18/00025 and DTS17/00145 (co-funded by *Fondo de Investigaciones Sanitarias of the Instituto de Salud Carlos III*, ISCIII, and the European Regional Development Fund, ERDF), (ii) RTI2018-094579-B-I00 (co-funded by *Ministerio de Ciencia, Innovación y Universidades*, Spain, and ERDF), and (iii) 2017-SGR-908 (*Generalitat de Catalunya*). GR was supported by a predoctoral fellowship from *VHIR – Amics del VHIR*. KAA is supported by an INPhINIT fellowship (LCF/BQ/DI18/11660061) from "La Caixa" Foundation (ID 100010434), with funding from European Union's Horizon 2020 Marie SkłodowskaCurie grant

agreement No. 713673. EdS is funded by a PERIS grant (SLT002/16/00316) from the Departament de Salut of the Generalitat de Catalunya (Spain). ASM is supported by a *Juan Rodés (JR18/00022)* postdoctoral fellowship from ISCIII. LNB-C was supported by the European Commission under Horizon 2020's Marie Skłodowska-Curie Actions COFUND scheme (712754) and by the Severo Ochoa program of the Spanish Ministry of Science and Competitiveness (SEV-2014-0425 (2015-2019)). Diagnostic Nanotools is a Consolidated Group supported by the *Secretaria d'Universitats i Recerca del Departament d'Empresa i Coneixement, Generalitat de Catalunya* (Grant 2017 SGR 240). ISGlobal and IBEC are members of the CERCA Program, *Generalitat de Catalunya*. This research is part of ISGlobal's Program on the Molecular Mechanisms of Malaria which is partially supported by *Fundación Ramón Areces*.

Bibliography

- Ashley, E.A., Pyae Phyo, A., Woodrow, C.J., 2018. Malaria. *Lancet*.
- Ben Ismail, M., de la Serna, E., Ruiz-Vega, G., García-Berrocso, T., Montaner, J., Zourob, M., Othmane, A., Baldrich, E., 2018. Using magnetic beads and signal amplifiers to produce short and simple immunoassays: Application to MMP-9 detection in plasma samples. *Anal. Chim. Acta* 999, 144–154.
- Bridger, N.A., Desai, S., Grimes, R., Hui, C.P.S., Mailman, T., Robinson, J.L., Salvadori, M., Vanderkooi, O.G., Allen, U.D., Audcent, T., Byington, C., Kropp, R., Le Saux, N., Moore, D.L., Mousmanis, P., 2015. The Committee to Advise on Tropical Medicine and Travel (CATMAT) ' a reference for Canadian paediatricians. *Paediatr. Child Heal.*
- De Souza Castilho, M., Laube, T., Yamanaka, H., Alegret, S., Pividori, M.I., 2011. Magneto immunoassays for plasmodium falciparum histidine-rich protein 2 related to malaria based on magnetic nanoparticles. *Anal. Chem.* 83, 5570–5577.
- Deraney, R.N., Mace, C.R., Rolland, J.P., Schonhorn, J.E., 2016. Multiplexed, Patterned-Paper Immunoassay for Detection of Malaria and Dengue Fever. *Anal. Chem.* 88, 6161–6165.
- Dincer, C., Bruch, R., Costa-Rama, E., Fernández-Abedul, M.T., Merkoçi, A., Manz, A., Urban, G.A., Güder, F., 2019. Disposable Sensors in Diagnostics, Food, and Environmental Monitoring. *Adv. Mater.*
- Fridley, G.E., Le, H., Yager, P., 2014. Highly sensitive immunoassay based on controlled rehydration of patterned reagents in a 2-dimensional paper network. *Anal. Chem.*
- Fu, E., Liang, T., Spicar-Mihalic, P., Houghtaling, J., Ramachandran, S., Yager, P., 2012. Two-dimensional paper network format that enables simple multistep assays for use in low-resource settings in the context of malaria antigen detection. *Anal. Chem.*
- GE Healthcare Bio-Sciences, 2013. Helping you build a smarter diagnostic assay Helping you build a smarter diagnostic assay. Marlborough, MA.
- Godino, N., Snakenborg, D., Kutter, J.P., Emnéus, J., Hansen, M.F., Muñoz, F.X., Javier Del Campo, F., 2010. Construction and characterisation of a modular microfluidic system: Coupling magnetic capture and electrochemical detection. *Microfluid. Nanofluidics*.
- Hänscheid, T., Grobusch, M.P., 2002. How useful is PCR in the diagnosis of malaria? *Trends Parasitol.*
- Jain, P., Chakma, B., Patra, S., Goswami, P., 2014. Potential Biomarkers and Their Applications for Rapid and Reliable Detection of Malaria. *Biomed Res. Int.* 2014, 852645.
- Jimenez, A., Rees-Channer, R.R., Perera, R., Gamboa, D., Chiodini, P.L., González, I.J., Mayor, A., Ding, X.C., 2017. Analytical sensitivity of current best-in-class malaria rapid diagnostic tests. *Malar. J.*

- Kasetsirikul, S., Buranapong, J., Srituravanich, W., Kaewthamasorn, M., Pimpin, A., 2016. The development of malaria diagnostic techniques: A review of the approaches with focus on dielectrophoretic and magnetophoretic methods. *Malar. J.*
- Kim, C., Searson, P.C., 2017. Detection of Plasmodium Lactate Dehydrogenase Antigen in Buffer Using Aptamer-Modified Magnetic Microparticles for Capture, Oligonucleotide-Modified Quantum Dots for Detection, and Oligonucleotide-Modified Gold Nanoparticles for Signal Amplification. *Bioconjug. Chem.*
- Kolluri, N., Klapperich, C.M., Cabodi, M., 2017. Towards lab-on-a-chip diagnostics for malaria elimination. *Lab Chip* 18, 75–94.
- Kosack, C.S., Page, A.L., Klatser, P.R., 2017. A guide to aid the selection of diagnostic tests. *Bull. World Health Organ.* 95, 639–645.
- Kozel, T.R., Burnham-Marusch, A.R., 2017. Point-of-Care Testing for Infectious Diseases: Past, Present, and Future. *J. Clin. Microbiol.*
- Ljungström, I., Moll, K., Perlmann, H., Scherf, A., Wahlgren, M., 2008. *Methods in malaria research.*
- Mahato, K., Srivastava, A., Chandra, P., 2017. Paper based diagnostics for personalized health care: Emerging technologies and commercial aspects. *Biosens. Bioelectron.* 96, 246–259.
- Maltha, J., Gillet, P., Jacobs, J., 2013. Malaria rapid diagnostic tests in endemic settings. *Clin. Microbiol. Infect.*
- Markwalter, C.F., Davis, K.M., Wright, D.W., 2016a. Immunomagnetic capture and colorimetric detection of malarial biomarker Plasmodium falciparum lactate dehydrogenase. *Anal. Biochem.*
- Markwalter, C.F., Ricks, K.M., Bitting, A.L., Mudenda, L., Wright, D.W., 2016b. Simultaneous capture and sequential detection of two malarial biomarkers on magnetic microparticles. *Talanta.*
- Mathison, B.A., Pritt, B.S., 2017. Update on Malaria Diagnostics and Test Utilization. *J. Clin. Microbiol.* 20, 49.
- Mayor, A., Serra-Casas, E., Bardají, A., Sanz, S., Puyol, L., Cisteró, P., Sigauque, B., Mandomando, I., Aponte, J.J., Alonso, P.L., Menéndez, C., 2009. Sub-microscopic infections and long-term recrudescence of Plasmodium falciparum in Mozambican pregnant women. *Malar. J.*
- McKenzie, F.E., Sirichaisinthop, J., Miller, R.S., Gasser, R.A., Wongsrichanalai, C., 2003. Dependence of malaria detection and species diagnosis by microscopy on parasite density. *Am. J. Trop. Med. Hyg.*
- Moles, E., Urbán, P., Jiménez-Díaz, M.B., Viera-Morilla, S., Angulo-Barturen, I., Busquets, M.A., Fernández-Busquets, X., 2015. Immunoliposome-mediated drug delivery to Plasmodium-infected and non-infected red blood cells as a dual therapeutic/prophylactic antimalarial strategy. *J. Control. Release.*
- Mukkala, A.N., Kwan, J., Lau, R., Harris, D., Kain, D., Boggild, A.K., 2018. An Update on Malaria Rapid Diagnostic Tests. *Curr. Infect. Dis. Rep.* 20, 49.
- Pereira, D.Y., Chiu, R.Y.T., Zhang, S.C.L., Wu, B.M., Kamei, D.T., 2015. Single-step, paper-based concentration and detection of a malaria biomarker. *Anal. Chim. Acta* 882, 83–89.
- Pham, N.M., Karlen, W., Beck, H.P., Delamarche, E., 2018. Malaria and the “last” parasite: How can technology help? *Malar. J.* 17, 260.
- Ragavan, K. V., Kumar, S., Swaraj, S., Neethirajan, S., 2018. Advances in biosensors and optical assays for diagnosis and detection of malaria. *Biosens. Bioelectron.* 105, 188–210.
- Rougemont, M., Van Saanen, M., Sahli, R., Hinrikson, H.P., Bille, J., Jaton, K., 2004. Detection of four Plasmodium species in blood from humans by 18S rRNA gene subunit-based and species-specific real-time PCR assays. *J. Clin. Microbiol.*
- Ruiz-Vega, G., Baldrich, E., 2017. Effect of agitation in magneto-assay performance. *Sensors Actuators, B Chem.* 247, 718–726.
- Ruiz-Vega, G., García-Robaina, A., Ben Ismail, M., Pasamar, H., García-Berrocó, T., Montaner,

- J., Zourob, M., Othmane, A., del Campo, F.J., Baldrich, E., 2018. Detection of plasma MMP-9 within minutes. Unveiling some of the clues to develop fast and simple electrochemical magneto-immunosensors. *Biosens. Bioelectron.* 115, 45–52.
- Ruiz-Vega, G., Kitsara, M., Pellitero, M.A., Baldrich, E., del Campo, F.J., 2017. Electrochemical Lateral Flow Devices: Towards Rapid Immunomagnetic Assays. *ChemElectroChem*.
- Salentijn, G.I.J., Grajewski, M., Verpoorte, E., 2018. Reinventing (Bio)chemical Analysis with Paper. *Anal. Chem.*
- WHO, 2018. World Malaria Report.
- WHO, 2015a. Global technical strategy for malaria, 2016-2030, WHO Geneva.
- WHO, 2015b. Malaria Rapid Diagnostic Test Performance. Results of WHO product testing of malaria RDTs: Round 6 (2014-2015), WHO Publications.
- Zarei, M., 2018. Infectious pathogens meet point-of-care diagnostics. *Biosens. Bioelectron.*
- Zarei, M., 2017. Portable biosensing devices for point-of-care diagnostics: Recent developments and applications. *TrAC, Trends Anal. Chem* 91, 26–41.

Electrochemical POC device for fast malaria quantitative diagnosis in whole blood by using magnetic beads, Poly-HRP and microfluidic paper electrodes

Supplementary Material

Gisela Ruiz-Vega^a, Kevin Arias-Alpizar^a, Erica de la Serna^a, Livia Neves Borgheti-Cardoso^{b,c}; Elena Sulleiro^{d,e}, Israel Molina^{e,f}, Xavier Fernández-Busquets^{b,c,g}, Adrián Sánchez-Montalvá^{e,f}, F. Javier del Campo^h, Eva Baldrich^{a,i}.

^a Diagnostic Nanotools Group, CIBBIM-Nanomedicine, Vall d'Hebron Research Institute (VHIR), Universitat Autònoma de Barcelona (UAB), Barcelona, Spain

^b Nanomalaria Group, Institute for Bioengineering of Catalonia (IBEC), The Barcelona Institute of Science and Technology (BIST), Barcelona, Spain

^c Barcelona Institute for Global Health (ISGlobal, Hospital Clínic-Universitat de Barcelona), Barcelona, Spain

^d Microbiology Department, Vall d'Hebron University Hospital (VHUH), UAB, Barcelona, Spain

^e PROSICS (Catalan International Health Program), Barcelona, Spain

^f Infectious Diseases Department, VHUH, UAB, PROSICS (Catalan International Health Program), Barcelona, Spain

^g Nanoscience and Nanotechnology Institute (IN2UB), Barcelona, Spain

^h Centro Nacional de Microelectrónica (IMB-CNM, CSIC), Barcelona, Spain

ⁱ CIBER de Bioingeniería, Biomateriales y Nanomedicina (CIBER-BBN), Spain

Material and Methods

P. falciparum in vitro cultures

The 3D7 *P. falciparum* strain was cultured at 37°C with group B human red blood cells (RBCs) at 3% hematocrit, following standard protocols (Ljungström et al., 2008). The human blood used was commercially obtained from the *Banc de Sang i Teixits* (www.bancsang.net) after having been discarded for transfusion, usually because of an excess of blood relative to anticoagulant solution. Prior to delivery, blood units were anonymized and irreversibly dissociated from the original database. The Ethical Committee on Clinical Research from the *Hospital Clínic de Barcelona* approved the study (Reg. HCB/2018/1223, January 23, 2019).

Parasites (thawed from glycerol stocks) were grown at 37 °C in Roswell Park Memorial Institute complete medium containing 5 g L⁻¹ AlbuMAX[®] II and 2 mM glutamine (RPMI-A, Invitrogen) under a gas mixture of 92.5% N₂, 5.5% CO₂, and 2% O₂. The medium was changed every 1-2 days maintaining 3% haematocrit. For culture maintenance, parasitemias were kept below 5% by dilution with fresh RBCs. For standard assays, parasitemia (unsynchronized parasites of mixed stages) was adjusted ranging from 0.0058 to 1.5% (45% haematocrit), obtained by serial dilution of the initial culture with fresh RBCs and medium.

Parasitemia of the initial culture was determined by flow cytometry using a BD LSRFortessa™ cell sorter (Becton, Dickinson and Company, Franklin Lakes, NJ, USA) (Moles et al., 2015) and the different culture dilutions were characterized by real-time PCR. For this, DNA from *P. falciparum* culture spots dried in filter paper was extracted using Chelex Method. Then, the DNA was amplified in an ABI PRISM 7500 HT Real-Time System (Applied Biosystems) as described by (Mayor et al., 2009). Each sample was run in triplicate and a negative-control sample with no template DNA was included in all plates. Parasitemia was quantified by extrapolation of cycle thresholds (Ct) from a standard curve of *P. falciparum* ring infected-RBCs. Samples without amplification (no Ct detected) were considered negative. Results were analyzed using ABI Prism software v2.0.6 (Applied Biosystems).

Figure S-1. Dimensions of the different MP-dsPCE components.

WE, working electrode; CE, counter electrode; RE pseudo-reference electrode; r, radius.

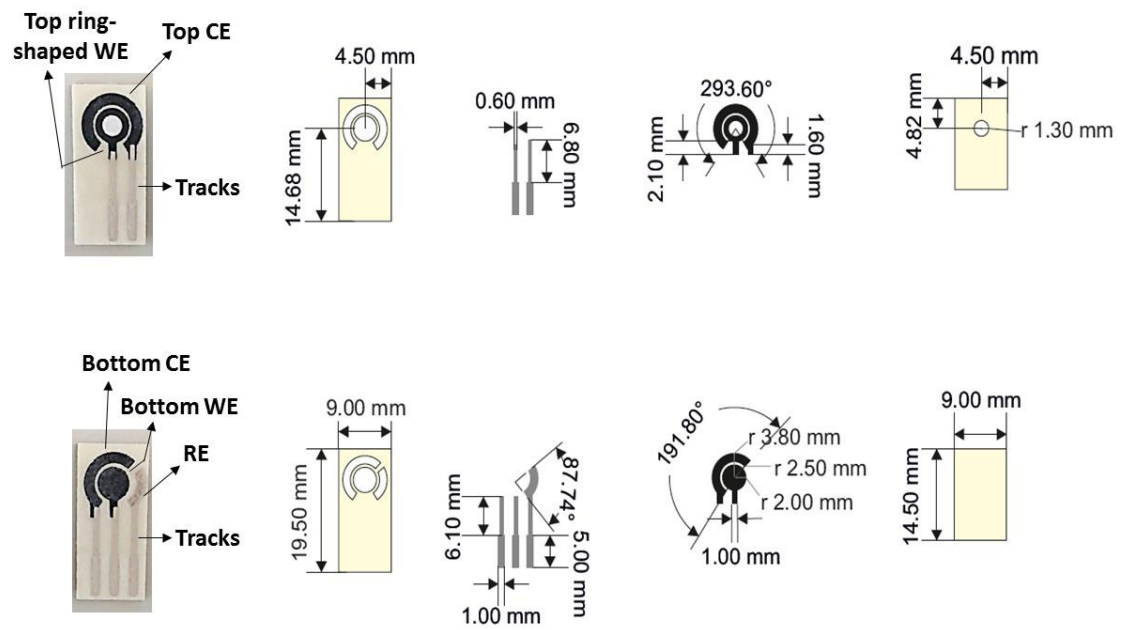


Figure S-2. Design and production of the MP-dsSPCE.

a) Masks used for double-sided screen printing. b) Photograph of both sides of the MP-dsSPCE. c) Scanning electron microscopy images of a transversal cut of the MP-dsSPCE carried at either the centre of the ring-shaped WE (left; conductive ink on the bottom of the chip) or at the double-sided WE (right; ink on both the top and bottom of the chip).

The procedure for MP-dsSPCE fabrication involved 8 printing steps. First, a layer of dielectric was printed. Next, the top carbon WE and CE were printed and cured (90 °C, 20 min). The silver tracks and contact pads were printed and cured (120 °C, 15 min). The tracks were then protected with a new dielectric coating. The Fusion 5 substrate was turned upside-down. A layer of dielectric UV curable dielectric paste was printed and the bottom WE and CE were printed and cured. The silver RE, tracks and contact pads were next printed and cured. Finally, the tracks were protected with a new dielectric coating. After printing, the Fusion 5 substrates were laser-cut into individual strips.

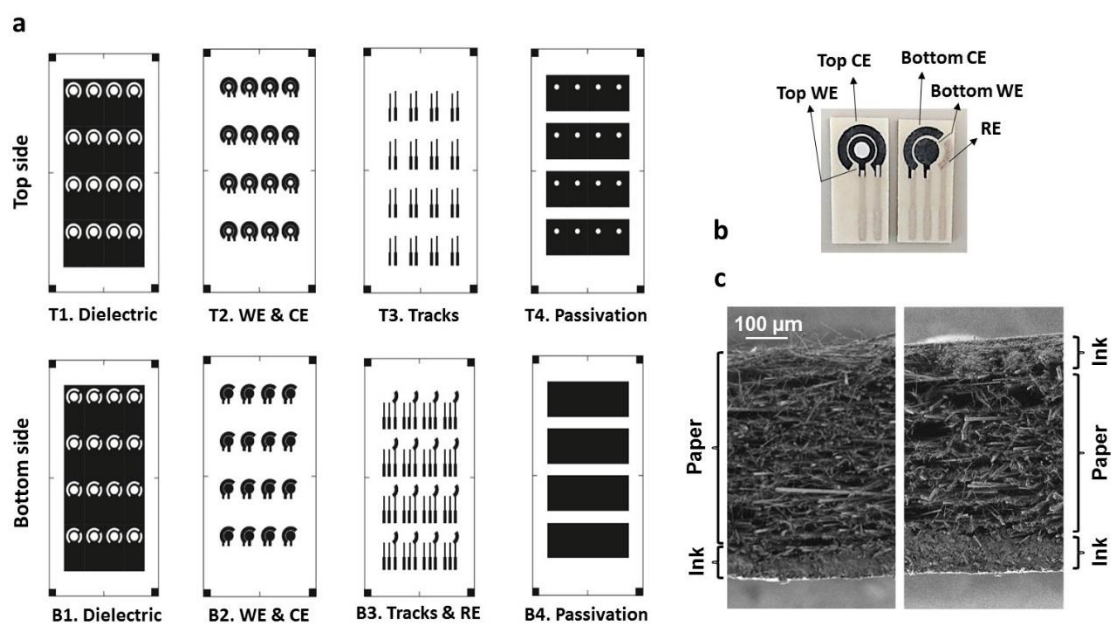


Figure S-3. Reproducibility of the production of bd-MAb/Poly-HRP.

Upon production, bd-MAb/Poly-HRP conjugates were tested in order to confirm their performance. For this, each production batch was used to study a positive control (100 ng mL⁻¹ of PflDH) and a negative control (no PflDH) using the colorimetric single-step sandwich magneto-immunoassay. The results obtained were then compared to those of conjugates from previous production batches (n=3 in all cases). The following table summarises the characterization experiments of 6 different batches of bd-MAb/Poly-HRP conjugates produced over time. As it can be observed, the signals obtained in the positive and negative controls were of the same order of magnitude (CV below 10%).

UA (450 nm)	[PflDH] (ng mL ⁻¹)	
	100	0
Batch 1	3.400	0.223
Batch 2	3.671	0.190
Batch 3	3.548	0.204
Batch 4	3.370	0.177
Batch 5	3.290	0.189
Batch 6	3.704	0.184
Aver	3.49	0.19
SD	0.17	0.011
CV	4.85	5.50

Figure S-4. Scheme and protocol of the classical sandwich ELISA for PflDH detection.

Unless otherwise stated, the incubations of the sandwich ELISA for PflDH detection were performed with 100 μL of solution per well, for 1 h each, inside an incubator thermostated at 37 $^{\circ}\text{C}$, and were followed by three washes with $\text{PBST}_{0.05\%}$ (200 μL per well). Briefly, microtiter plates were modified with the corresponding c-Ab (2.5 $\mu\text{g mL}^{-1}$ of PflDH-c-MAb, in PBS) and were blocked with $\text{PBST}_{0.05\%}$ -BSA $_{1\%}$. After washing, the plates were incubated with 0.0016-100 ng mL^{-1} of PflDH in $\text{PBST}_{0.05\%}$ -BSA $_{1\%}$. Plates were next incubated with 37.5 ng mL^{-1} of PLDH-bd-MAb in $\text{PBST}_{0.05\%}$ -BSA $_{1\%}$. Finally, the plates were incubated at room temperature with strep-HRP (1:200 in $\text{PBST}_{0.05\%}$ -BSA $_{1\%}$) for 20 min. After four more washes, the plates were incubated for 20 min at room temperature with TMB- H_2O_2 substrate solution and were detected using an ELISA plate reader.

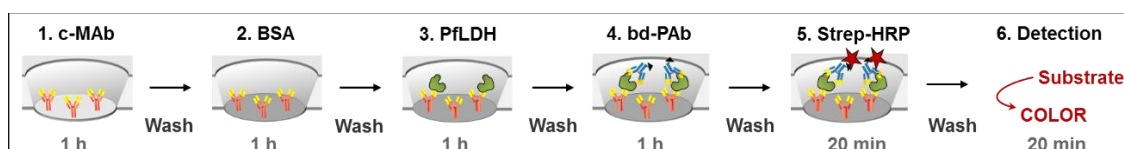


Figure S-5. Photograph of the MP-dsSPCE plugged to a standard double-sided 2.54 mm pitch connector.

To carry out a measurement under static (a) conditions, a drop of solution was placed onto the electrochemical cell. In flow conditions (b), a stack of adsorbent pads was placed in contact with the frontal edge of the chip to provide solution drainage, and the whole assembly was placed inside a segment of electrical cable trunking, used here as a physical holder.



Figure S-6. Impermeabilization of the MP-dsSPCE connectors.

In order to prevent solution passage upstream from the MP-dsSPCE and into the electrical connector, the connecting paths were treated with a transparent impermeabilizing solution (Rubson SX9000, Henkel, Germany), which was stained for these experiments. This economical product, which is sold for the impermeabilization of building materials, was acquired at a local retailer. First, we investigated the volume of water repellent necessary to penetrate only the area of interest, without affecting the electrochemical cell. For this, several MP-dsSPCE were inserted in the wells of a 96-well microtiter plate, containing increasing volumes of impermeabilizing solution. When all the solution had been adsorbed, the MP-dsSPCE were recovered and were dried for 3 h in an incubator at 37 °C. The two sides of the chips were then stripped from each other. As it can be observed in the image, 15 μL of solution were needed to protect completely the connector paths. Higher volumes, on the other hand, provided irregular paper protection, often affecting the areas that displayed the electrodes.

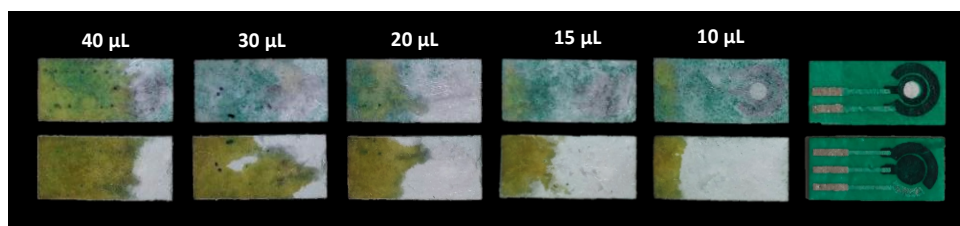


Figure S-7. Characteristics of the different membranes tested in this work for the production of an absorbent pad for the MP-dsSPCE.

(-) indicates that this data was not facilitated by the supplier.

Membrane	Material	Properties	Lateral flow application	Thickness (μm)	Wicking rate (s/4cm)	Water absorption (mg cm^{-2})
LF1	Bound glass fibre	Works well with whole blood or serum samples and can act as a blood separator as well	Blood separation	247	35.6	25.3
MF1			Blood separation	367	29.7	39.4
VF2			Blood separation	785	23.8	86.2
Standard 17		Faster flow than cotton, with lower sample retention	Conjugate release	370	34.5	44.9
GF/DVA		Works well with saliva samples and can act as a blood separator also	Blood separation	785	28.2	93
CF5	100% cotton linter	Medium weight	Absorption pad	954	63.3	99.2
CF4			Sample application & absorption pad	482	67.3	49.9
Fusion 5	Glass fibre with a plastic binder	Can be used as a lateral flow blood separator	Blood separation & conjugate release	370	38.0	40
Prima 40	Nitrocellulose	Works as a backed membrane, increasing mechanical strength	Backed reservoir pad for saliva	192	44.0	-

Figure S-8. Study of the absorption capacity of different membranes.

The nine types of membranes described in Figure S-7 (GE Healthcare) were evaluated for the production of an absorbent pad for the MP-dsSPCE. For this study, 100 μL of methylene blue were pipetted on one edge of 4 \times 1 cm membrane strips and the distance run by the solution was measured. CF5, GF/DVA and VF2 provided the highest absorption capacity, which was consistent with the data facilitated by the provider (99.2, 93 and 86.2 mg cm^{-2} , respectively). Of them, CF5 displayed more homogeneous flow and was selected for the production of the MP-dsSPCE absorption pad.

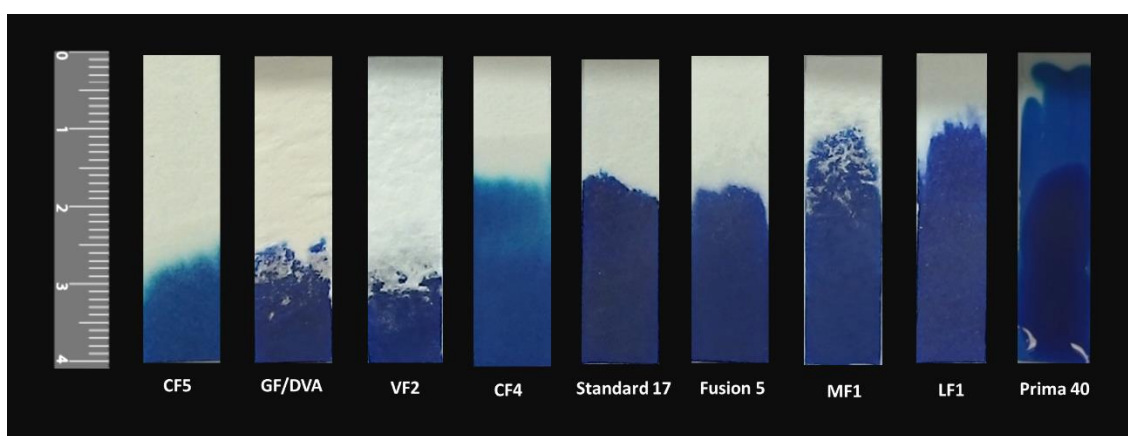


Figure S-9. Optimization of a 2-step magneto-immunoassay for PflDH detection.

a) Scheme of the assay. b) Signals registered for different MB concentrations per sample during the magneto-immunoassay. c) Signals registered using different concentrations of bd-MAb per sample. d) Optimization of Poly-HRP concentration. The zoomed bars correspond to the background signals registered in the negative control experiments (without PflDH). In all cases, the inserts display the *S/N* ratios at low PflDH concentrations and the LOD/LOQ for the corresponding graphs. The main graphs display averages of at least three replicates and their standard deviations. The best results were obtained for 20 μg of MB per 100- μL sample (75 ng mL^{-1} of bd-MAb and 50 ng mL^{-1} of Poly-HRP).

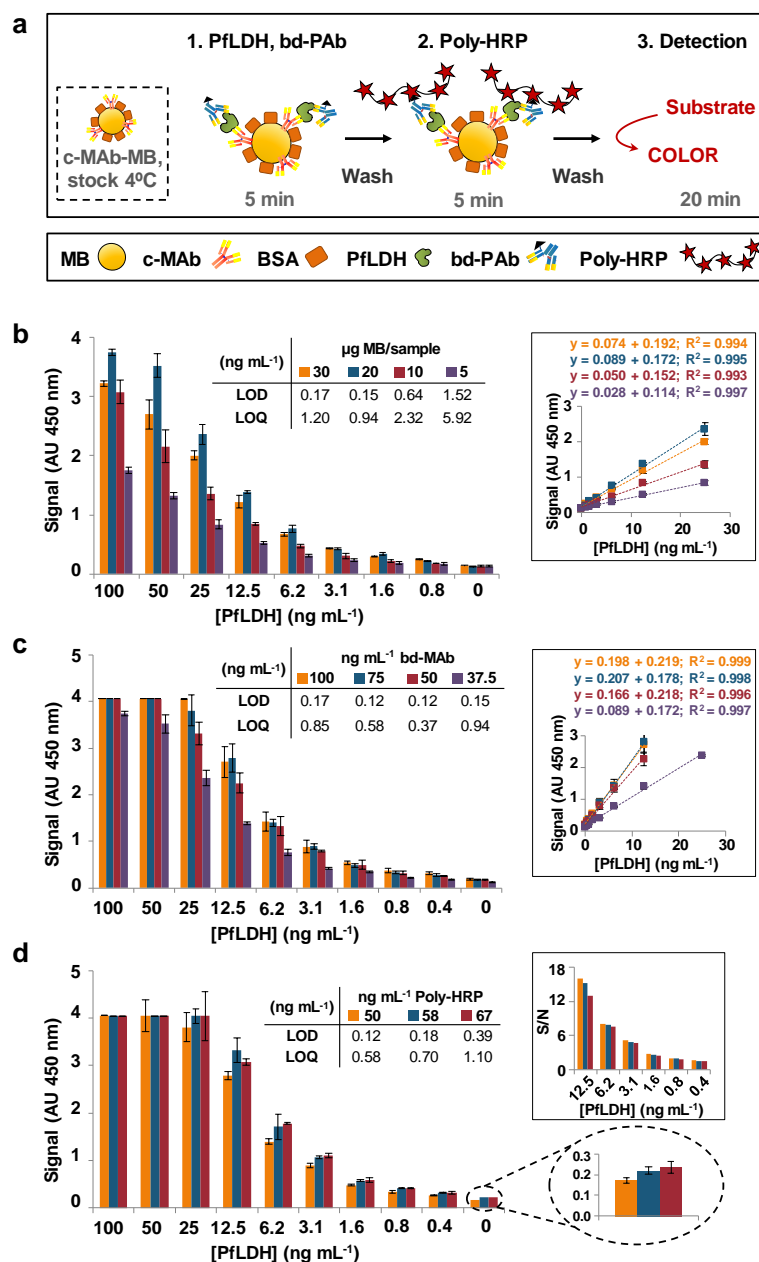


Figure S-10. Optimization of Poly-HRP immunoconjugate preparation and optimization of the single step magneto-immunoassay for PflDH detection.

Linear range (n=3) (a), signal-to-noise ratios (S/N) (b), and figures of merit (c) of the single-step magneto-immunoassay using bd-MAb/Poly-HRP conjugates prepared with a fixed concentration of 50 ng mL⁻¹ for Poly-HRP and different amounts of bd-MAb.

The lowest LOD and LOQ were obtained for the highest concentrations of PLDH-bd-MAb, 225 ng mL⁻¹ and 300 ng mL⁻¹, and the concentration selected was 225 ng mL⁻¹ to reduce the assay cost. Among the different immunoconjugate dilutions studied the best performance was achieved for 225 ng mL⁻¹ of PLDH-bd-MAb and 50 ng mL⁻¹ of Poly-HRP. Finally, the incubation time of Poly-HRP with PLDH-bd-Mab was optimized and the signals registered for 60 min incubation time showed the best LOD and LOQ and lower background noise and variability.

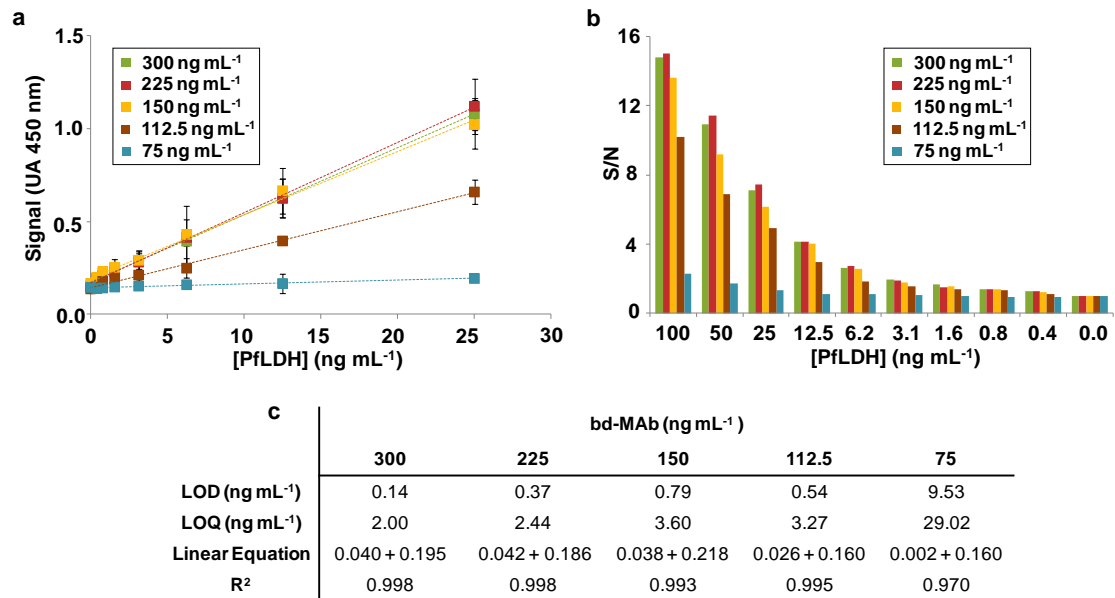


Figure S-11. Optimization of the electrochemical measurement conditions using the MP-dsSPCE under either static (a-c) or flow (d-f) conditions.

The whole assay was performed in tubes in the absence or in the presence of PfLDH (12.5 and 100 ng mL⁻¹). After the last wash, MB were resuspended in 100 μL of TMB-H₂O₂ substrate solution and were pipetted on the MP-dsSPCE to perform the detection on-chip. Detection was then performed at different potentials (a, d), using increasing volumes of substrate solution (b, e) or employing different MB concentrations per sample (c, f). The results are discussed in the main manuscript.

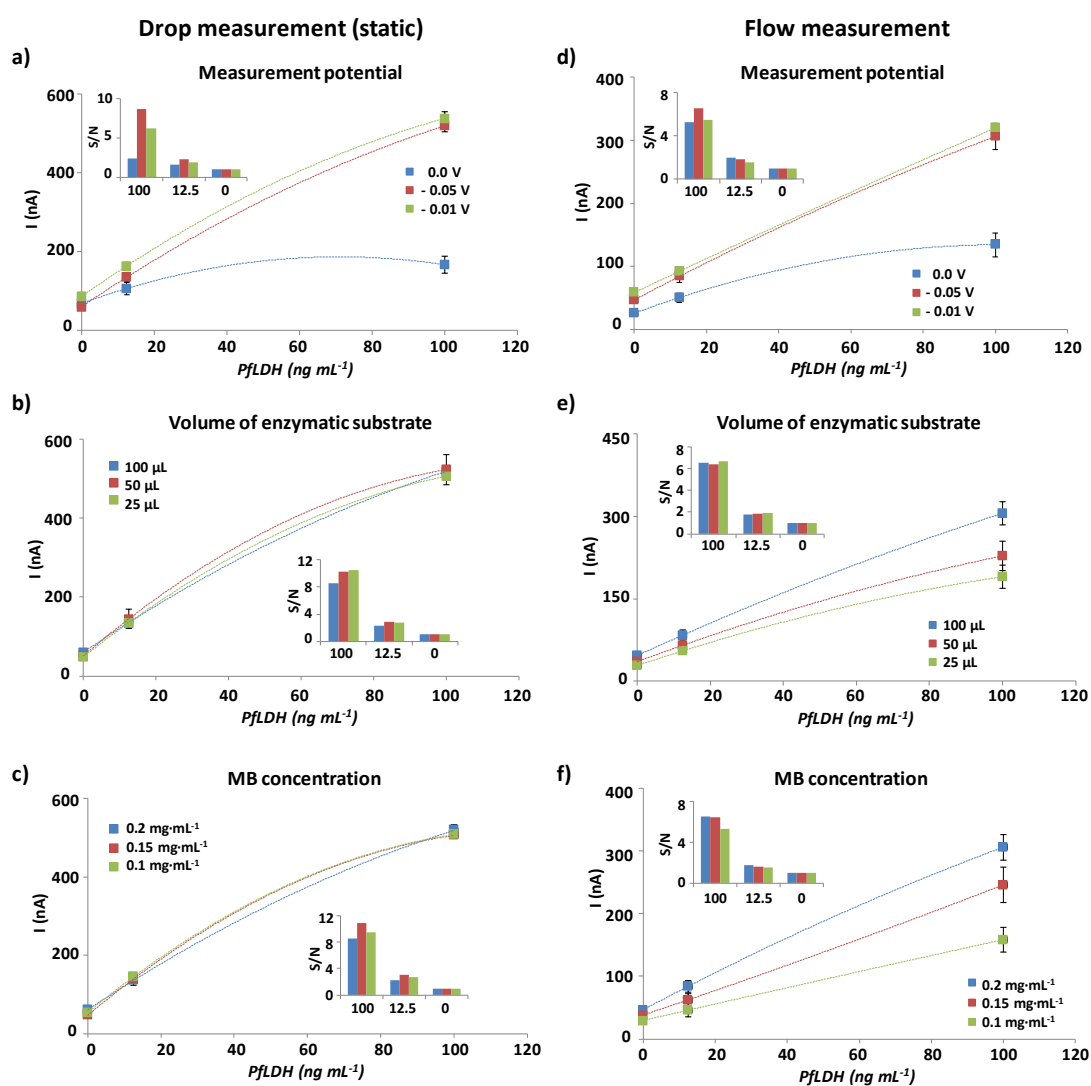


Figure S-12. Effect of the anticoagulant in PfLDH detection using the colorimetric single-step magneto-immunoassay.

The applicability of the single-step magneto-immunoassay developed was assessed by studying its performance in whole blood. Whole blood samples were obtained in collection tubes containing anticoagulant in order to facilitate blood handling and storage. However, because blood thinners may interfere in assay performance (Bowen and Remaley, 2014), the potential effect of different anticoagulants on magneto-immunoassay performance was first examined. With this purpose, whole blood was obtained from a healthy individual using 3 different blood thinners (ethylenediaminetetraacetic acid (EDTA), acid-citrate-dextrose (ACD), and heparin), or no anticoagulant at all. Each blood sample was then assayed using the single-step magneto-immunoassay, before and after spiking 100 ng mL⁻¹ of PfLDH (n=3). As it can be observed, EDTA interfered in assay performance and produced unacceptably high background noise. On the other hand, heparin-treated blood produced the lowest level of interference in the immunoassay, providing the signals and S/N ratios that better resembled those obtained in fresh blood without anticoagulant.

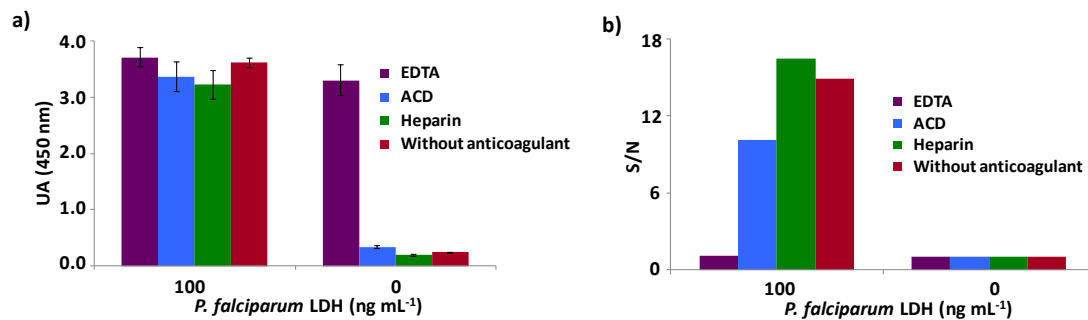


Figure S-13. Design and assembly of the blood filter unit that was incorporated to the washing system of the MP-dsSPCE for the study of lysed whole blood.

The device developed was a Fusion 5 strip (30×10 mm) with a protruding star-like fringe. The latter included in the centre a circular section of similar diameter than the top WE. When placed onto the MP-dsSPCE, this section behaved as a MB retention zone and prevented sample entry through the orifice in the top WE into the MP-dsSPCE by directing the flow towards the main body of the filtration unit, which acted as both flow pump and waste container.

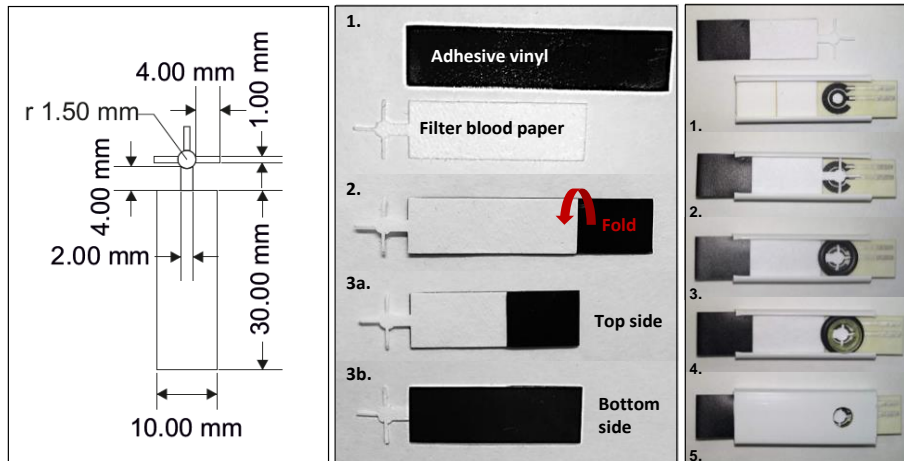


Figure S-14. Reproducibility of the reported method.

The magneto-immunosensor proposed was evaluated by detecting increasing concentrations of PflLDH spiked in lysed whole blood. After the 5-min single-step incubation with c-MAb-MB and bd-MAb/Poly-HRP conjugate, the mixture was directly pipetted on a cartridge displaying a filtration unit, which was followed by on-chip washing and detection. Alternatively, MB were concentrated with a magnet and the solution was removed by pipetting. MB were next resuspended in PBS and were pipetted on a cartridge for on-chip washing and detection. As it can be observed in the table, after manual cell debris elimination using a magnetic rack the assay displayed result variability (CV) that was in average of 7.04 % (blood dilution 1:25) and 6.92 %CV (blood dilution 1:50). Alternative on-chip sample filtration using the device and method reported here produced result variability that was in average of 8.85 % (blood dilution 1:25) and 11.16 % (blood dilution 1:50). These values were below 15% in all cases, which are the maximal values accepted for diagnostic applications.

[PflLDH] ng mL ⁻¹	CV (n=3)			
	Debris magnetic removal	Debris magnetic removal	Debris filtered on-chip	Debris filtered on-chip
	Blood 1:25	Blood 1:50	Blood 1:25	Blood 1:50
100	9.20	5.50	9.62	13.10
50	5.86	4.92	11.72	10.97
25	11.05	9.11	10.44	10.89
12	5.05	4.61	7.61	11.78
6	3.83	8.32	5.89	10.22
0	7.24	9.05	7.81	7.99
Average CV	7.04	6.92	9.85	10.82

Figure S-15. Detection of PfLDH in *P. falciparum*-infected RBC cultures with controlled parasitemias.

Plot of the concentrations of PfLDH (ng mL⁻¹) estimated by the MP-dsSPCE versus the concentrations detected by the reference ELISA (a), the magneto-immunosensor detected using commercial SPCE (b), and the parasitemia estimated in the original culture by microscopy and flow cytometry (c).

RBCs were infected *in vitro* with controlled *P. falciparum* parasitemias (spanning 0.0058-1.5%, equivalent to 340-87209 p μL⁻¹). Samples were then lysed for 5 min, diluted 1:25 with PBST-BSA_{1%}, and evaluated in parallel by the magneto-immunosensor using MP-dsSPCE, ELISA, PCR, and flow cytometry. The concentrations of PfLDH estimated by the MP-dsSPCE correlated linearly with those provided by the reference ELISA (positive lineal Pearson correlation coefficient of 0.97) and the microscopic observation (positive lineal Pearson correlation coefficient of 0.93). Interestingly, the results provided by the MP-dsSPCE based sensor correlated as well with those obtained if the magneto-immunosensor was detected using classical washes in tubes and detection at commercial SPCE (positive lineal Pearson correlation coefficient of 0.99), which confirmed that the washes performed on-chip were efficient.

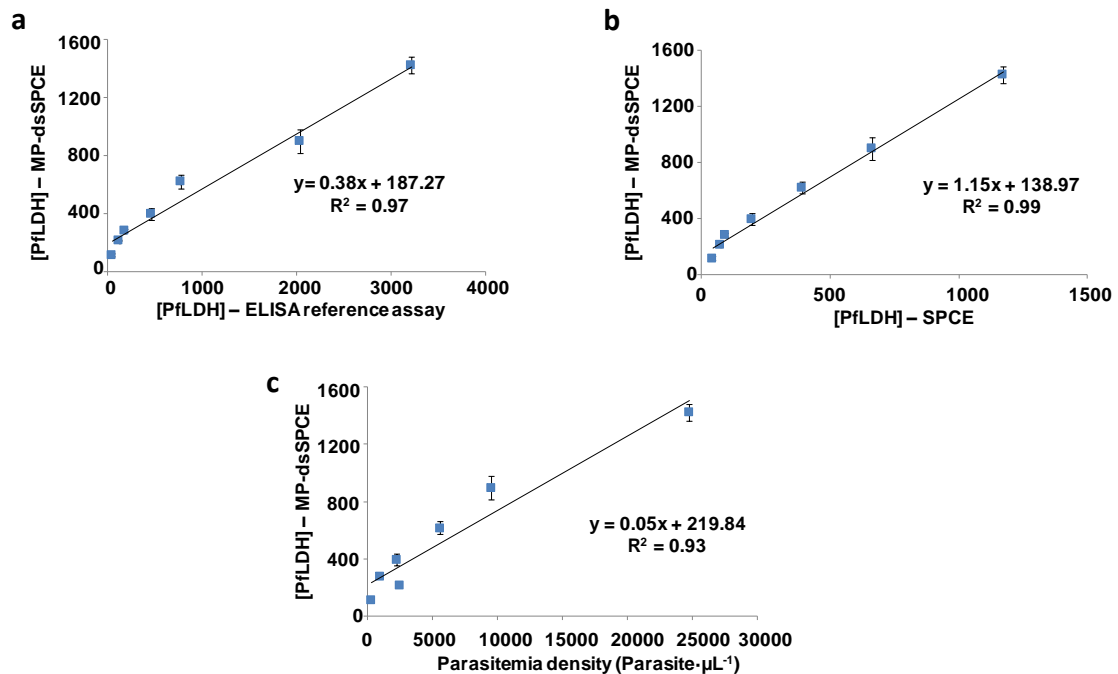
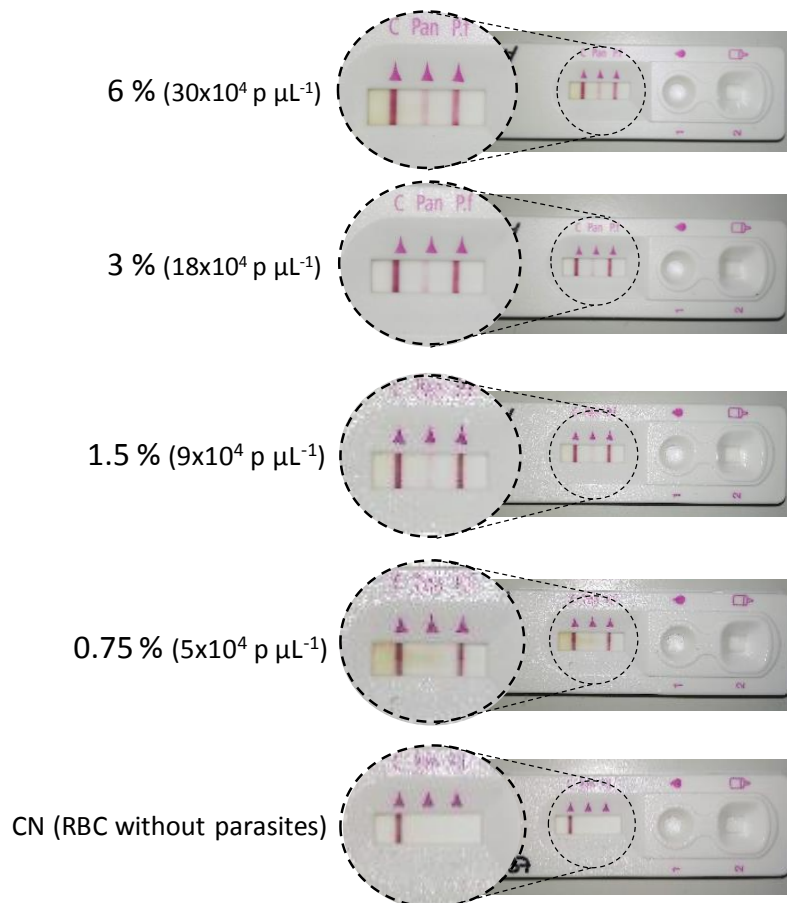


Figure S-16. PfLDH detection using one of the commercial RDTs recommended by the WHO.

PfLDH was detected in cultured RBCs infected *in vitro* with controlled *P. falciparum* parasitemias using the SD BIOLINE Malaria Ag P.f/Pan Screening test, provided by Standard Diagnostics – Alere (now Abbot). Samples were handled and processed following the instructions provided by the supplier.

This commercial RDT displayed, from left to right, a control line, a line for *Plasmodium* LDH, and a band for *P. falciparum* HRP2. As it can be observed, LDH detection was significantly less sensitive than HRP2 detection. Specifically, the device provided negative results for PAN LDH in samples with 0.75% parasitemia, faint LDH positives for parasitemias of 1,5% and 3%, and clear LDH positives only for parasitemias above 6%.



Bibliography

- Bowen, R.A.R., Remaley, A.T., 2014. Interferences from blood collection tube components on clinical chemistry assays. *Biochem. Medica* 24, 31–44.
- Ljungström, I., Moll, K., Perlmann, H., Scherf, A., Wahlgren, M., 2008. Methods in malaria research, Malaria Research and Reference Reagent Resource Center (MR4).
- Mayor, A., Serra-Casas, E., Bardají, A., Sanz, S., Puyol, L., Cisteró, P., Sigauque, B., Mandomando, I., Aponte, J.J., Alonso, P.L., Menéndez, C., 2009. Sub-microscopic infections and long-term recrudescence of *Plasmodium falciparum* in Mozambican pregnant women. *Malar. J.* 8, 9.
- Moles, E., Urbán, P., Jiménez-Díaz, M.B., Viera-Morilla, S., Angulo-Barturen, I., Busquets, M.A., Fernández-Busquets, X., 2015. Immunoliposome-mediated drug delivery to *Plasmodium*-infected and non-infected red blood cells as a dual therapeutic/prophylactic antimalarial strategy. *J. Control. Release* 210, 217–229.